Steric Effects in the Binding of Hindered Dibenzothiophene Ligands in $[Cp'Ru(CO)_2(\eta^1(S)\text{-DBTh})]^+$ Complexes

Paul A. Vecchi, Arkady Ellern,† and Robert J. Angelici*

Ames Laboratory and Department of Chemistry, Iowa State University, Ames, Iowa 50011

Received December 29, 2004

Structural studies of several complexes of the type $[Cp'Ru(CO)_2(\eta^1(S)\text{-DBTh})]^+$, where Cp′ = Cp or Cp* and DBTh = DBT, 4-MeDBT, 4,6-Me_2DBT, or 2,8-Me_2DBT, show that only in $[Cp^*Ru(CO)_2(\eta^1(S)\text{-4,6-}Me_2DBT)]^+$ is there evidence for steric crowding between the Cp′ and DBTh ligands. However, relative equilibrium constants (K') for the binding of the DBTh ligands in both the Cp and Cp* complexes show evidence of steric effects in those that contain 4-MeDBT and 4,6-Me_2DBT as the K' values increase in the order 4,6-Me_2DBT < 4-MeDBT < DBT < 2,8-Me_2DBT. Kinetics studies of the substitution of the DBTh in $[CpRu(CO)_2(\eta^1\text{-}(S)\text{-DBTh})]^+$ by phosphorus donor ligands establish the following order of DBTh lability, 4,6-Me_2DBT > 4-MeDBT > DBT > 2,8-Me_2DBT, which is consistent with the trend in K' values. The most labile DBTh ligand in both series of complexes is 4,6-Me_2DBT in $[Cp^*Ru\text{-}(CO)_2(\eta^1(S)\text{-4,6-}Me_2DBT)]^+$, where both steric crowding and electron donation by the Cp* ligand accelerate the rate of 4,6-Me_2DBT dissociation.

Introduction

The removal of organosulfur compounds from petroleum feedstocks is important for the reduction of atmospheric pollution caused by sulfur oxides.[1] Sulfur compounds in these fuels also poison catalytic converters, impairing the vehicle emission control systems necessary to reduce levels of nitrogen oxides released into the atmosphere during fuel combustion. In addressing these issues, the United States government through the Environmental Protection Agency (EPA) has gradually established lower sulfur limits in transportation fuels.[2]

Sulfur is currently removed from gasoline and diesel fuels using a catalytic process known as hydrodesulfurization (HDS). The most difficult of the sulfur-containing compounds to be removed using HDS are the hindered dibenzothiophene derivatives (DBTh) that contain alkyl groups near the sulfur in the 4- and 6-positions (Figure 1).[1a,3] These dibenzothiophene compounds are found in diesel fuel and must be removed in order to lower its sulfur content. Although it is unclear exactly how dibenzothiophenes interact with the catalyst surface during HDS, it has been proposed that an initial step is binding of the substrate through the sulfur atom to active metal sites.[4] The slow rates for the HDS of 4-methyldibenzothiophene (4-MeDBT) and 4,6-dimethyldibenzothiophene (4,6-Me_2DBT) have been attributed to steric hindrance by methyl groups in the 4,6-positions that interfere with their binding to such sites. Alkyl groups in these positions have also been proposed to sterically hinder C−S bond cleavage during HDS.[5] Improvements in the HDS process have not adequately addressed the difficulties of desulfurizing hindered dibenzothiophenes.

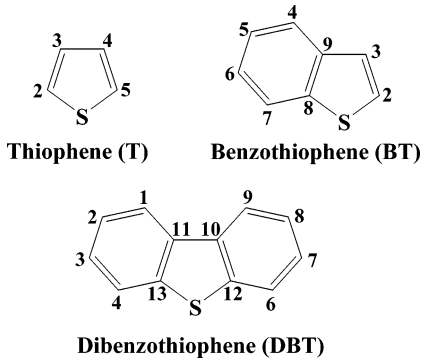

Figure 1. Numbering schemes for the aromatic thiophene (T), benzothiophene (BT), and dibenzothiophene (DBT) compounds found in petroleum feedstocks.

* To whom correspondence should be addressed. E-mail: angelici@iastate.edu.

† Molecular Structure Laboratory, Iowa State University, Ames, IA 50011.

(1) (a) Whitehurst, D. D.; Isoda, T.; Mochida, I. *Adv. Catal.* **1998**, *42*, 345. (b) Angelici, R. J. In *Encyclopedia of Inorganic Chemistry*; King, R. B., Ed.; Wiley & Sons: New York, 1994; p 1433. (c) Kasztelan, S.; Des Courieres, T.; Breysse, M. *Catal. Today* **1991**, *10*, 433. (d) Ho, T. C. *Catal. Rev.* **1988**, *30*, 117.

(2) (a) Connell, C. *Fed. Regist.* **2000**, *65*, 6697. (b) Borushko, M. *Fed. Regist*. **2001**, *66*, 5001.

(3) (a) Ho, T. C. *Catal. Today* **2004**, *98*, 3. (b) Song, C.; Ma, X. *Appl. Catal., B* **2003**, *41*, 207. (c) Gates, B. C.; Topsøe, H. *Polyhedron* **1997**, *16*, 3213.

(4) (a) Topsøe, H.; Clausen, B. S.; Massoth, F. E. *Hydrotreating Catalysis. Science and Technology;* Springer-Verlag: Berlin, 1996. (b) Chianelli, R. R.; Pecoraro, T. A.; Halbert, T. R.; Pan, W. H.; Stiefel, E. I. *J. Catal*. **1984**, *86*, 226. (c) Pecoraro, T. A.; Chianelli, R. R. *J. Catal*. **1981**, *67*, 430.

(5) (a) Mijoin, J.; Perot, G.; Bataille, F.; Lemberton, J.-L.; Breysse, M.; Kasztelan, S. *Catal. Lett.* **2001**, *71*, 139. (b) Bataille, F.; Lemberton, J.-L.; Michaud, P.; Perot, G.; Vrinat, M.; Lemaire, M.; Schulz, E.; Breysse, M.; Kasztelan, S. *J. Catal.* **2000**, *191*, 409. (c) Meille, V.; Schulz, E.; Lemaire, M.; Vrinat, M. *J. Catal.* **1997**, *170*, 29. (d) Kabe, T.; Ishihara, A.; Zhang, Q. *Appl. Catal., A* **1993**, *97*, L1.

10.1021/om048973l CCC: $30.25
Publication on Web 03/31/2005

Recently, the focus has shifted away from improving current HDS processes toward developing new technologies for desulfurization.[3,6] One promising new method is the use of adsorbents or solid phase extractants (SPEs) to selectively bind and remove sulfur compounds such as the hindered dibenzothiophenes.[3,6−8] Adsorbent technologies have the potential advantage of being relatively simple to incorporate into the existing infrastructure as either a pre- or post-HDS treatment. Such treatments may also be designed to operate under relatively mild conditions, unlike HDS, which currently involves the use of moderately high temperatures (350−500 °C) and pressures (50−150 psi) of hydrogen. Another emerging technology for desulfurization of hydrocarbon fuels is catalytic oxidation of hindered dibenzothiophenes to the sulfones or sulfoxides, which can then be removed by extraction or adsorption.[9] In both of these new desulfurization approaches, an important step involves binding of the dibenzothiophene to either the adsorbent or catalyst.

Several experimental and theoretical studies on the binding of thiophenes, benzothiophenes, and dibenzothiophenes to transition metal complexes have been reported.[10] However, there are comparatively few experimental studies of hindered dibenzothiophenes that are $\eta^1(S)$-coordinated in metal complexes,[11] presumably a result of the instability of such complexes. An understanding of the relative bond strengths and kinetic labilities of hindered dibenzothiophenes in metal complexes should be useful for developing new approaches to petroleum feedstock desulfurization. We recently reported the synthesis and structural characterization of the first transition metal complexes of $\eta^1(S)$-bound 4-MeDBT and 4,6-Me_2DBT, $[Cp^*Ru(CO)_2(\eta^1(S)$-4-MeDBT$)]^+$ and $[Cp^*Ru(CO)_2(\eta^1(S)$-4,6-Me_2DBT$)]^+$, where $Cp^* = \eta^5$-C_5Me_5.[11] Equilibrium studies of the displacement of 4,6-Me_2DBT in $[Cp^*Ru(CO)_2(\eta^1(S)$-4,6-Me_2DBT$)]^+$ by the dibenzothiophenes (DBTh) DBT, 4-MeDBT, and 2,8-Me_2DBT (eq 1) showed that their binding abilities increase in the following order: 4,6-Me_2DBT (1.00) < 4-MeDBT (20.2(1)) < DBT (62.7(6)) < 2,8-Me_2DBT (223(3)). In this report, we continue our investigations of sulfur-bound dibenzothiophenes, with special attention directed toward understanding the role of steric and electronic effects in both the $[CpRu(CO)_2(\eta^1$-(S)-DBTh$)]^+$ and $[Cp^*Ru(CO)_2(\eta^1(S)$-DBTh$)]^+$ series of complexes (where Cp = η^5-C_5H_5, and DBTh = DBT, 4-MeDBT, 4,6-Me_2DBT, and 2,8-Me_2DBT). Equilibrium binding constants and rates of DBTh substitution for these complexes provide insight into factors that influence the thermodynamic and kinetic binding of 4- and 4,6-methyl-substituted dibenzothiophenes to $\{Cp'Ru(CO)_2\}^+$, where Cp′ = Cp and Cp*.

$$[Cp^*Ru(CO)_2(\eta^1(S)\text{-}4,6\text{-}Me_2DBT)]^+ + DBTh \underset{CD_2Cl_2}{\overset{25.0\ ^\circ C}{\rightleftharpoons}} [Cp^*Ru(CO)_2(\eta^1(S)\text{-}DBTh)]^+ + 4,6\text{-}Me_2DBT \quad (1)$$

Experimental Section

General Considerations. All reactions were performed under an atmosphere of dry argon using standard Schlenk techniques. Methylene chloride (CH_2Cl_2), diethyl ether (Et_2O), and hexanes were purified on alumina using a Solv-Tek solvent purification system, similar to that described by Grubbs and co-workers.[12] Nitromethane (CH_3NO_2, 96+%) was purchased from Aldrich and subjected to three freeze−pump−thaw cycles before use. Acetone was stirred with calcium chloride overnight, distilled, subjected to three freeze−pump−thaw cycles, and stored under argon until use. Methylene chloride-d_2 (CD_2Cl_2) was refluxed overnight with calcium hydride, distilled, subjected to three freeze−pump−thaw cycles, and stored under argon until use. Nitromethane-d_3 (CD_3NO_2) was purchased from Aldrich, subjected to three freeze−pump−thaw cycles, and stored under argon before use. Solid DBT and 4-MeDBT were purchased from Aldrich and sublimed prior to use. Solid 4,6-Me_2DBT and 2,8-Me_2DBT were purchased from Acros and TCI, respectively, and used without further purification. Compounds $AgBF_4$ (99.99+%), $P(OPh)_3$, PPh_3, and PPh_2Me were purchased from Aldrich and used without further purification. Complexes $CpRu(CO)_2Cl$,[13] $[CpRu(CO)_2(\eta^1$-(S)-DBT$)]BF_4$ (**1**),[14] and $[Cp^*Ru(CO)_2(\eta^1$-(S)-DBTh$)]^+$ (DBTh = DBT (**5**), 4-MeDBT (**6**), 4,6-Me_2DBT (**7**), 2,8-Me_2DBT (**8**))[11] were prepared as described previously.

Filtrations were performed with Celite on filter paper. Solution NMR spectra were recorded on a Bruker DRX-400 spectrometer using either CD_2Cl_2 ($\delta = 5.32$ (^{1}H), 54.0 (^{13}C)) or CD_3NO_2 ($\delta = 4.33$ (^{1}H), 62.8 (^{13}C)) as the solvent, internal lock, and reference. Solution infrared spectra of the compounds in CH_2Cl_2 were recorded on a Nicolet-560 spectrometer using NaCl cells with 0.1 mm spacers. Elemental analyses were performed on a Perkin-Elmer 2400 series II CHNS/O analyzer.

General Procedure for Preparation of the $[CpRu(CO)_2(\eta^1(S)$-DBTh$)]BF_4$ Complexes (2−4). To a solution of $CpRu(CO)_2Cl$ (75 mg, 0.291 mmol) and 0.320 mmol of DBTh (DBTh = 4-MeDBT, 4,6-Me_2DBT, 2,8-Me_2DBT) in 10 mL of CH_2Cl_2 was added solid $AgBF_4$ (58.4 mg, 0.300 mmol), and the solution was stirred at room temperature under argon for 30 min. A solid precipitate formed and the yellow solution color gradually lightened during the reaction. The reaction solution was then filtered and transferred by cannula into a flask containing 40 mL of diethyl ether in an ice water bath, which resulted in precipitation of the product. The remaining solid in the reaction flask was washed with a 1 mL portion of CH_3NO_2, and the solution was also transferred by cannula into the diethyl ether to ensure complete transfer of the product. The light yellow solid products were isolated by filtration and washed with three 5 mL portions of diethyl ether to remove excess DBTh. Isolated yields were typically 70−85%. Due to

(6) Song, C. *Catal. Today* **2003**, *86*, 211.
(7) (a) Hernandez-Maldonado, A. J.; Yang, R. T. *J. Am. Chem. Soc.* **2004**, *126*, 992. (b) Yang, F. H.; Hernandez-Maldonado, A. J.; Yang, R. T. *Sep. Sci. Technol.* **2004**, *39*, 1717. (c) Haji, S.; Erkey, C. *Ind. Eng. Chem. Res.* **2003**, *42*, 6933. (d) Hernandez-Maldonado, A. J.; Yang, R. T. *Ind. Eng. Chem. Res.* **2003**, *42*, 3103. (e) Yang, R. T.; Hernandez-Maldonado, A. J.; Yang, F. H. *Science* **2003**, *301*, 79. (f) Velu, S.; Ma, X.; Song, C. *Ind. Eng. Chem. Res.* **2003**, *42*, 5293. (g) Ma, X.; Sun, L.; Song, C. *Catal. Today* **2002**, *77*, 107. (h) Kobayashi, M.; Shirai, H.; Nunokawa, M. *Energy Fuels* **2002**, *16*, 1378. (i) McKinley, S. G.; Angelici, R. J. *Energy Fuels* **2003**, *17*, 1480.
(8) McKinley, S. G.; Vecchi, P. A.; Ellern, A.; Angelici, R. J. *Dalton Trans.* **2004**, *5*, 788.
(9) (a) Murata, S.; Murata, K.; Kidena, K.; Nomura, M. *Energy Fuels* **2004**, *18*, 116. (b) Wang, D.; Qian, E. W.; Amano, H.; Okata, K.; Ishihara, A.; Kabe, T. *Appl. Catal., A* **2003**, *253*, 91. (c) Wang, Y.; Lente, G.; Espenson, J. H. *Inorg. Chem.* **2002**, *41*, 1272. (d) Te, M.; Fairbridge, C.; Ring, Z. *Appl. Catal., A* **2001**, *219*, 267.
(10) For reviews see: (a) Sánchez-Delgado, R. A. *Organometallic Modeling of the Hydrodesulfurization and Hydrodenitrogenation Reactions*; Kluwer Academic Publishers: Dordrecht, Netherlands, 2002. (b) Angelici, R. J. *Organometallics* **2001**, *20*, 1259. (c) Chen, Jiabi; Angelici, R. J. *Coord. Chem. Rev.* **2000**, *206−207*, 63. (d) Harris, S. *Polyhedron* **1997**, *16*, 3219. (e) Angelici, R. J. *Coord. Chem. Rev.* **1990**, *105*, 61.
(11) Vecchi, P. A.; Ellern, A.; Angelici, R. J. *J. Am. Chem. Soc.* **2003**, *125*, 2064.
(12) Pangborn, A. B.; Giardello, M. A.; Grubbs, R. H.; Rosen, R. K.; Timmers, F. J. *Organometallics* **1996**, *15*, 1518.
(13) Eisenstadt, A.; Tannenbaum, R.; Efraty, A. *J. Organomet. Chem.* **1981**, *221*, 317.
(14) Benson, J. W.; Angelici, R. J. *Organometallics* **1993**, *12*, 680.

Table 1. Crystal Data and Structure Refinement for 2, 3, and 4

	[CpRu(CO)$_2$(η^1(*S*)-4-MeDBT)]BF$_4$ (**2**)	[CpRu(CO)$_2$(η^1(*S*)-4,6-Me$_2$DBTh)]BF$_4$ (**3**)	[CpRu(CO)$_2$(η^1(*S*)-2,8-Me$_2$DBTh)]BF$_4$ (**4**)
empirical formula	$C_{20}H_{15}BF_4O_2RuS$	$C_{21}H_{17}BF_4O_2RuS$	$C_{21}H_{17}BF_4O_2RuS$
fw	507.26	521.29	521.29
temperature	173(2) K	293(2) K	173(2) K
wavelength	0.71073 Å	0.71073 Å	0.71073 Å
cryst syst	monoclinic	triclinic	monoclinic
space group	*P*2(1)/*c*	$P\bar{1}$	*P*2(1)/*n*
unit cell dimens	*a* = 11.699(4) Å *b* = 12.520(5) Å *c* = 13.149(5) Å α = 90.0° *β* = 94.534(6)° *γ* = 90.0°	*a* = 9.3637(8) Å *b* = 10.4141(9) Å *c* = 11.7381(9) Å α = 73.448(1)° *β* = 69.504(1)° *γ* = 88.382(2)°	*a* = 9.394(4) Å *b* = 11.003(5) Å *c* = 19.963(9) Å α = 90.000° *β* = 98.660(8)° *γ* = 90.000°
volume	1920.0(12) Å^3	1024.48(15) Å^3	2039.7(16) Å^3
Z	4	2	4
cryst color, habit	yellow plate	yellow prism	yellow prism
density (calcd)	1.755 Mg/m^3	1.690 Mg/m^3	1.698 Mg/m^3
abs coeff	0.977 mm^{-1}	0.918 mm^{-1}	0.922 mm^{-1}
F(000)	1008	520	1040
cryst size	0.20 × 0.20 × 0.10 mm^3	0.30 × 0.28 × 0.21 mm^3	0.30 × 0.30 × 0.23 mm^3
θ range for data collection	1.75 to 25.00°	1.94 to 26.37°	2.06 to 28.29°
index ranges	$-13 \le h \le 13$ $-13 \le k \le 14$ $-15 \le l \le 14$	$-11 \le h \le 11$ $-13 \le k \le 8$ $-14 \le l \le 14$	$-11 \le h \le 12$ $-14 \le k \le 14$ $-26 \le l \le 26$
no. of reflns collected	13 529	6757	19 275
no. of ind reflns	3341 [*R*(int) = 0.0422]	4112 [*R*(int) = 0.0183]	4706 [*R*(int) = 0.0394]
completeness to *θ* =	25.00° = 98.8%	26.37° = 98.1%	28.29° = 99.0%
abs corr	semiempirical from equivalents	empirical with SADABS	semiempirical from equivalents
max. and min. transmn	0.44 and 0.31	0.86 and 0.76	1.00 and 0.88
refinement method	full-matrix least-squares on F^2	full-matrix least-squares on F^2	full-matrix least-squares on F^2
no. of data/restraints/params	3341/0/262	4112/0/271	4706/0/271
goodness-of-fit on F^2	1.100	1.013	1.221
final R^a indices [$I > 2\sigma(I)$]	R1 = 0.0677 wR2 = 0.2007	R1 = 0.0311 wR2 = 0.0777	R1 = 0.0787 wR2 = 0.1936
R^a indices (all data)	R1 = 0.0744 wR2 = 0.2085	R1 = 0.0380 wR2 = 0.0805	R1 = 0.0833 wR2 = 0.1956
largest diff peak and hole	4.094 and −0.874 e Å^{-3}	0.785 and −0.782 e Å^{-3}	2.792 and −1.822 e Å^{-3}

[a] $R1 = \sum||F_o| - |F_c||/\sum|F_o|$ and $wR2 = \{\sum[w(F_o^2 - F_c^2)^2]/\sum[w(F_o^2)^2]\}^{1/2}$.

the low solubility of the products in methylene chloride, ^{1}H NMR and ^{13}C NMR spectra were acquired in CD_3NO_2. Spectroscopic data for compound **1** were reported previously.[14]

Characterization of Compounds 2−4. [CpRu(CO)$_2$(η^1-(*S*)-4-MeDBT)][BF$_4$] (2). ^{1}H NMR (400 MHz, CD_3NO_2): *δ* 8.29−8.26 (m, 1H), 8.18 (d, *J* = 7.6 Hz, 1H), 8.05−8.03 (m, 1H), 7.76−7.69 (m, 3H), 7.51 (d, *J* = 7.6 Hz, 1H), 2.64 (s, 3H, CH_3), 4-MeDBT; 5.79 (s, 5H), Cp. ^{13}C NMR (100.6 MHz, CD_3NO_2): *δ* 194.53 (CO); 142.98, 140.22, 138.79, 138.31, 136.44, 131.85, 131.69, 131.13, 131.06, 126.67, 124.80, 122.62, 21.42 (4-MeDBT); 91.37 (Cp). IR (CH_2Cl_2): *ν*(CO) (cm^{-1}) 2076(s), 2033(s). Anal. Calcd for $C_{20}H_{15}BF_4O_2RuS$: C, 47.35; H, 2.98; S, 6.32. Found: C, 47.16; H, 2.95; S, 6.28.

[CpRu(CO)$_2$(η^1(*S*)-4,6-Me$_2$DBT)][BF$_4$] (3). ^{1}H NMR (400 MHz, CD_3NO_2): *δ* 8.12 (d, *J* = 7.6 Hz, 2H), 7.69 (t, *J* = 7.6 Hz, 2H), 7.50 (d, *J* = 7.6 Hz, 2H), 2.62 (s, 6H, CH_3), 4,6-Me$_2$-DBT; 6.02 (s, 5H), Cp. ^{13}C NMR (100.6 MHz, CD_3NO_2): *δ* 194.15 (CO); 141.23, 138.87, 135.94, 131.89, 131.49, 122.66, 21.39 (4,6-Me$_2$DBT); 91.28 (Cp). IR (CH_2Cl_2): *ν*(CO) (cm^{-1}) 2076(s), 2033(s). Anal. Calcd for $C_{21}H_{17}BF_4O_2RuS$: C, 48.38; H, 3.29; S, 6.15. Found: C, 47.98; H, 3.43; S, 6.04.

[CpRu(CO)$_2$(η^1(*S*)-2,8-Me$_2$DBT)][BF$_4$] (4). ^{1}H NMR (400 MHz, CD_3NO_2): *δ* 8.08 (s, 2H), 7.85 (d, *J* = 8.4 Hz, 2H), 7.52 (d, *J* = 8.4 Hz, 2H), 2.56 (s, 6H, CH_3), 2,8-Me$_2$DBT; 5.82 (s, 5H), Cp. ^{13}C NMR (100.6 MHz, CD_3NO_2): *δ* 194.63 (CO); 142.17, 139.02, 138.48, 131.74, 126.40, 124.91, 21.65 (2,8-Me$_2$-DBT); 91.16 (Cp). IR (CH_2Cl_2): *ν*(CO) (cm^{-1}) 2076(s), 2032(s). Anal. Calcd for $C_{21}H_{17}BF_4O_2RuS$: C, 48.38; H, 3.29; S, 6.15. Found: C, 47.99; H, 3.46; S, 6.04.

X-ray Structural Determinations of [CpRu(CO)$_2$(η^1(*S*)-4-MeDBT)][BF$_4$] (2), [CpRu(CO)$_2$(η^1(*S*)-4,6-Me$_2$DBT)][BF$_4$] (3), and [CpRu(CO)$_2$(η^1(*S*)-2,8-Me$_2$DBT)][BF$_4$] (4). A yellow single crystal of **2** suitable for an X-ray diffraction study was obtained by slow cooling of a saturated CH_2Cl_2 solution of the complex at −25 °C for 1 week. A yellow single crystal of **3** suitable for an X-ray diffraction study was obtained by layering a saturated CH_2Cl_2 solution of the complex with Et_2O under argon and storing at −25 °C for 1 week. Crystals of **4**, also yellow, were obtained by preparing an acetone solution of the complex, filtering it through Celite, and allowing it to slowly evaporate in air at room temperature.

The crystals were selected under ambient conditions, coated in epoxy, and mounted on the end of a glass fiber. Crystal data collection was performed on a Bruker CCD-1000 diffractometer with Mo Kα (*λ* = 0.71073 Å) radiation and a collector-to-crystal distance of 5.03 cm. Cell constants were determined from a list of reflections found by an automated search routine. Data were collected using the full sphere routine and were corrected for Lorentz and polarization effects. The absorption corrections were based on fitting a function to the empirical transmission surface as sampled by multiple equivalent measurements using SADABS software.[15] Positions of the heavy atoms were found by the Patterson method. The remaining atoms were located in an alternating series of least-squares cycles and difference Fourier maps. All non-hydrogen atoms were refined in full-matrix anisotropic approximation. All hydrogen atoms were placed in the structure factor calculation at idealized positions and refined using a riding model. Complete data collection and reduction information for each compound are given in Table 1.

Equilibrium Studies. Solutions for the equilibrium studies (eq 2) were prepared by placing 0.020 mmol of [CpRu(CO)$_2$-

(15) Blessing, R. H. *Acta Crystallogr.* **1995** A*51*, 33.

Table 2. Ru−S Bond Distances (Å) and Twist Angles (deg) for [CpRu(CO)$_2$(η^1(*S*)-DBTh)][BF$_4$] Complexes 1−4 and for the [Cp*Ru(CO)$_2$(η^1(*S*)-DBTh)][BF$_4$] Complexes 5−7

complex	Ru−S distance (Å)	twist angle (deg)
[CpRu(CO)$_2$(η^1(*S*)-DBT)]$^+$ [a] (**1**)	2.398(2)	22.8
[CpRu(CO)$_2$(η^1(*S*)-4-MeDBT)]$^+$ [b] (**2**)	2.377(2)	8.6
[CpRu(CO)$_2$(η^1(*S*)-4,6-Me$_2$DBT)]$^+$ [b] (**3**)	2.405(1)	8.9
[CpRu(CO)$_2$(η^1(*S*)-2,8-Me$_2$DBT)]$^+$ [b] (**4**)	2.400(1)	25.0
[Cp*Ru(CO)$_2$(η^1(*S*)-DBT)]$^+$ [c] (**5**)	2.394(1)	20.2
[Cp*Ru(CO)$_2$(η^1(*S*)-4-MeDBT)]$^+$ [c] (**6**)	2.399(1), 2.404(1)	11.3, 12.3
[Cp*Ru(CO)$_2$(η^1(*S*)-4,6-Me$_2$DBT)]$^+$ [c] (**7**)	2.419(1)	0.4

[a] Reference 8. [b] This study. [c] Reference 11.

Table 3. Equilibrium Constants, *K*, for Reactions (eq 2) of [CpRu(CO)$_2$(η^1(*S*)-DBTh)]$^+$ with DBTh′ at 25.0 °C in CD$_3$NO$_2$

DBTh	DBTh′	*K*
DBT	4-MeDBT	0.358(8)
DBT	4,6-Me$_2$DBT	0.103(2)
DBT	2,8-Me$_2$DBT	3.77(3)
4-MeDBT	4,6-Me$_2$DBT	0.344(15)

(η^1(*S*)-DBTh)][BF$_4$] (DBTh = DBT, 4-MeDBT, 4,6-Me$_2$DBT, 2,8-Me$_2$DBT) and an equimolar amount of a different dibenzothiophene (DBTh′) in a 5 mm NMR tube. Approximately 0.7

$$[\mathrm{CpRu(CO)_2}(\eta^1(S)\text{-DBTh})]^+ + \mathrm{DBTh}' \underset{\mathrm{CD_3NO_2,\ 25.0\ °C}}{\overset{K}{\rightleftharpoons}} [\mathrm{CpRu(CO)_2}(\eta^1(S)\text{-DBTh}')]^+ + \mathrm{DBTh} \quad (2)$$

mL of CD_3NO_2 was added to dissolve the reactants, and the reaction solution was frozen in liquid nitrogen. After degassing, the solution was thawed and flame-sealed under argon at room temperature. The tube was then placed in a circulating bath thermostated at 25.0 ± 0.1 °C, and the reaction progress was monitored periodically by ^{1}H NMR spectroscopy using CD_3NO_2 as the internal lock and reference (δ = 4.33) with a 10 s pulse delay between scans to ensure complete relaxation of proton signals. Equilibrium constants (*K*) were calculated from the ^{1}H NMR spectra using eq 3,

$$K = \frac{(I_{\mathrm{Cp}}'/5)^2}{(I_{\mathrm{Cp}}/5)^2} = \frac{[\mathrm{CpRu(CO)_2}(\eta^1(S)\text{-DBTh}')]^+[\mathrm{DBTh}]}{[\mathrm{CpRu(CO)_2}(\eta^1(S)\text{-DBTh})]^+[\mathrm{DBTh}']} \quad (3)$$

where I_{Cp}' and I_{Cp} are the Cp peak integrals of [CpRu(CO)$_2$(η^1(*S*)-DBTh′)]$^+$ and [CpRu(CO)$_2$(η^1(*S*)-DBTh)]$^+$, respectively. All equilibria were established from both reaction directions by separate experiments, and the results (Table 3) are the average of the forward and reverse reactions with the average deviation given in parentheses. All equilibria were established within 10 days, and no further changes in the ^{1}H NMR spectra were observed when examined after 14 days. Equilibrium constants for analogous reactions of the [Cp*Ru(CO)$_2$(η^1(*S*)-DBTh)][BF$_4$] complexes (DBTh = DBT, 4-MeDBT, 4,6-Me$_2$DBT, 2,8-Me$_2$DBT) were reported previously.[11]

Kinetic Studies. Solutions of [CpRu(CO)$_2$(η^1(*S*)-DBTh)][BF$_4$] (DBTh = DBT, 4-MeDBT, 4,6-Me$_2$DBT, 2,8-Me$_2$DBT) for kinetic studies were prepared according to the following procedure: A 0.010 mmol sample of the complex was added to an NMR tube, and the tube was evacuated and flushed with argon. Deoxygenated CD_3NO_2 was added, followed by a measured excess of P(OPh)$_3$ so that the total volume of the reaction mixture was 0.50 mL. The tube was capped with a septum, shaken to dissolve the reactants, and placed in a circulating bath thermostated at 25.0 ± 0.1 °C. At periodic intervals, the reaction tube was removed and monitored by ^{1}H NMR spectroscopy using CD_3NO_2 as the internal lock and reference (δ = 4.33). Typically 8−12 spectra were collected over 2−3 half-lives for each reaction. The products formed during the course of the kinetic reactions were [CpRu(CO)$_2$(P(OPh)$_3$)]$^+$ [16] and the free dibenzothiophenes (eq 4), which were identified by their NMR spectra. Relative concentrations of reactants and

$$[\mathrm{Cp'Ru(CO)_2}(\eta^1(S)\text{-DBTh})]^+ + \mathrm{PR_3} \xrightarrow[25.0\ °C]{k_{\mathrm{obs}}} [\mathrm{Cp'Ru(CO)_2(PR_3)}]^+ + \mathrm{DBTh} \quad (4)$$

Cp′ = η^5-C$_5$H$_5$; PR$_3$ = P(OPh)$_3$, PPh$_3$;
Cp′ = η^5-C$_5$Me$_5$; PR$_3$ = PPh$_3$, PPh$_2$Me

products were determined by integration of the ^{1}H NMR signals for either the Cp or DBTh ligands. Rate constants, k_{obs}, were obtained from the least-squares slopes of plots of ln(1 + *F*) (where *F* = [product]/[reactant]) versus time, and the correlation coefficients of these plots were always greater than 0.995.

Solutions of [Cp*Ru(CO)$_2$(η^1(*S*)-DBTh)][BF$_4$] (DBTh = DBT, 4-MeDBT, 4,6-Me$_2$DBT, 2,8-Me$_2$DBT) for the kinetic studies were prepared in a slightly different manner. A 0.010 mmol sample of the complex was added to an NMR tube with an excess, weighed amount of PPh$_3$. The tube was then evacuated and flushed with argon. A 0.50 mL aliquot of CD_2Cl_2 was added; the tube was capped with a septum and shaken to dissolve the reactants. The tube was immediately placed into the probe of a Bruker DRX-400 spectrometer thermostated at 25.0 ± 0.1 °C. The spectrometer was preprogrammed to acquire ^{1}H NMR spectra at specific time intervals using CD_2Cl_2 as the internal lock and reference (δ = 5.32); the acquisition time to take each spectrum was 60 s (16 scans at 3.744 s/scan). Typically 8−12 spectra were collected over 2−3 half-lives for each reaction. The products formed during the course of these kinetic reactions were [Cp*Ru(CO)$_2$(PPh$_3$)]$^+$ [17] and the free dibenzothiophenes (eq 4), which were identified by their NMR spectra. Relative concentrations of reactants and products were determined by integration of methyl groups on the Cp* and/or DBTh ligands. Rate constants, k_{obs}, were obtained as described above, and the correlation coefficients of these plots were always greater than 0.995. Reactions with the liquid phosphine PPh$_2$Me were undertaken in the same manner, except that the phosphine was injected by syringe immediately after the deuterated solvent had been added. The ruthenium product, [Cp*Ru(CO)$_2$(PPh$_2$Me)]$^+$, gave an ^{1}H NMR spectrum (for PPh$_2$*Me*, δ = 2.27, d, ^3J(P,H) = 9.3 Hz, 3H; for Cp*, δ = 1.87, d, *J*(P,H) = 2.0 Hz, 15H) that is similar to that of [Cp*Ru(CO)$_2$(PPh$_3$)]$^+$. The amount of deuterated solvent in each reaction was calibrated to ensure that the total volume of each reaction solution was 0.50 mL.

Results and Discussion

Synthesis of the [CpRu(CO)$_2$(η^1(*S*)-DBTh)][BF$_4$] Complexes. The complexes [CpRu(CO)$_2$(η^1(*S*)-DBTh)][BF$_4$], where DBTh = DBT (**1**), 4-MeDBT (**2**), 4,6-Me$_2$DBT (**3**), and 2,8-Me$_2$DBT (**4**), are prepared by Cl$^-$ abstraction from CpRu(CO)$_2$Cl with AgBF$_4$ in the presence of excess dibenzothiophene ligand in CH_2Cl_2 (eq 5). Complexes **1**−**4** are isolated as air-stable, pale yellow powders that are insoluble in diethyl ether and hexanes,

$$\mathrm{CpRu(CO)_2Cl} + \mathrm{DBTh} \xrightarrow[\text{RT, 30 min, } -\mathrm{AgCl}]{\mathrm{AgBF_4,\ CH_2Cl_2}} [\mathrm{CpRu(CO)_2}(\eta^1(S)\text{-DBTh})][\mathrm{BF_4}] \quad (5)$$

minimally soluble in CH_2Cl_2 and acetone, and soluble in CH_3NO_2. ^{1}H NMR data show that the signals of the DBTh ligands in these complexes are shifted slightly downfield of the free ligand signals, as is observed in other $\eta^1(S)$ complexes of dibenzothiophene.[8,11,18] If the DBTh ligand were bound η^2 through a C=C bond or η^6 to one of the arene rings, one would expect to see significant upfield ^{1}H and ^{13}C NMR shifts for signals of the coordinated groups, as are observed for η^2-olefin[19] and η^6-arene complexes of ruthenium.[20] The IR spectra of these complexes in CH_2Cl_2 exhibit two ν(CO) signals (2076, 2033 cm^{-1}) that are essentially the same for all four compounds and are on average 25 cm^{-1} higher than those (ν(CO) = 2056, 2004 cm^{-1} in CH_2Cl_2) of the $CpRu(CO)_2Cl$ starting material. The ^{13}C NMR spectrum for $[CpRu(CO)_2(\eta^1(S)\text{-4-MeDBT})]^+$ (**2**) has only one signal for the two diastereotopic carbonyl ligands at room temperature, indicating that there is a dynamic process at room temperature that makes the CO groups equivalent on the ^{13}C NMR time scale. This process is likely to involve rapid inversion at the sulfur atom. Due to the poor solubility of **2** in CD_2Cl_2, THF-d_6, and $(CD_3)_2$-CO, NMR studies of the complex were limited to temperatures above the freezing point of CD_3NO_2 (244 K), where inversion remained rapid. In previous studies of related complexes, the $\Delta G^{\ddagger}$ barriers to inversion were determined for $[CpRu(CO)_2(\eta^1(S)\text{-BT})]^+$ (43 kJ/mol at 205 K; BT = benzothiophene),[14] $[CpRu(CO)(PPh_3)(\eta^1(S)\text{-Th})]^+$ (40 kJ/mol at 213 K; Th = 2,5-Me_2T and Me_4T),[18a] and $[CpFe(CO)_2(\eta^1(S)\text{-BT})]^+$ (39 kJ/mol at 190 K).[18b]

Structures of Compounds 2, 3, and 4. In all of the structures (Figure 2) of the $[CpRu(CO)_2(\eta^1(S)\text{-DBTh})][BF_4]$ (**2**−**4**) complexes, the DBTh ligands are η^1-coordinated through a pyramidal sulfur atom, and the DBTh ligand is oriented away from the Cp ligand, as has been observed in other cationic complexes containing $\eta^1(S)$-bound dibenzothiophene ligands: $[CpRu(CO)_2(\eta^1(S)\text{-DBT})][BF_4]$,[8] $[Cp^*Ru(CO)_2(\eta^1(S)\text{-DBTh}][BF_4]$ (where DBTh = DBT, 4-MeDBT, 4,6-Me_2DBT),[11] and $[CpFe(CO)_2(\eta^1(S)\text{-DBT})][BF_4]$.[18b] The Ru−S distances (Table 2) for complexes **1**,[8] **2**, **3**, and **4** are 2.398(2), 2.377(2), 2.405(1), and 2.400(2) Å, respectively. All of these values are very similar to each other except in complex **2**, which has a shorter Ru−S bond than the other complexes. The orientation of the DBTh ligand around the Ru−S bond may be defined by the dihedral angle Cp(centroid)−Ru−S−midpoint between C(10) and C(11). For a symmetrical orientation, this angle would be 180°, and the deviation from 180° is defined as the twist angle. In compounds **1**, **2**, **3**, and **4**, this angle is 22.8°, 8.6°, 8.9°, and 25.0°, respectively (Table 2). These angles indicate that there is some degree of rotational freedom around the Ru−S bond in all of the complexes, even in the 4,6-Me_2DBT complex (**3**).

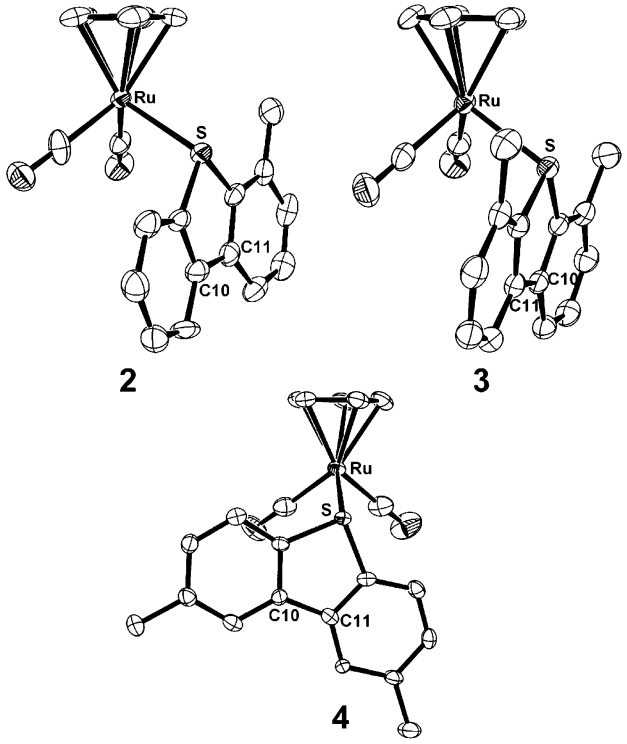

Figure 2. Thermal ellipsoid drawings of the cations in $[CpRu(CO)_2(\eta^1(S)\text{-4-MeDBT})][BF_4]$ (**2**), $[CpRu(CO)_2(\eta^1(S)\text{-4,6-Me}_2\text{DBT})][BF_4]$ (**3**), and $[CpRu(CO)_2(\eta^1(S)\text{-2,8-Me}_2\text{DBT})][BF_4]$ (**4**). Ellipsoids are shown at the 50% probability level; hydrogen atoms are omitted for clarity.

Thus, there is no structural evidence for steric crowding caused by the 4,6-methyl groups in the $[CpRu(CO)_2(\eta^1(S)\text{-DBTh})]^+$ complexes **1**−**4**. This is in contrast to a previous structural investigation of the series of $[Cp^*Ru(CO)_2(\eta^1(S)\text{-DBTh})]^+$ complexes,[11] where DBTh = DBT, 4-MeDBT, and 4,6-Me_2DBT, in which methyl groups in both the 4- and 4,6-positions affect significantly the structures of these complexes. In that study, the Ru−S distance (Table 2) increased with the number of 4,6-methyl groups as follows: DBT (2.394(1)) ≤ 4-MeDBT (2.399(1), 2.404(1))[21] < 4,6-Me_2DBT (2.419(1)). The lengthening of the Ru−S bond, especially for the 4,6-Me_2DBT complex, was attributed to steric repulsions between methyl groups on the DBTh ligand and Cp* methyl groups. The twist angles for the $[Cp^*Ru(CO)_2(\eta^1(S)\text{-DBTh})]^+$ complexes (Table 2) decrease with an increasing number of 4,6-methyl groups: DBT (20.2°) > 4-MeDBT (11.3°, 12.3°) > 4,6-Me_2DBT (0.4°). Especially in $[Cp^*Ru(CO)_2(\eta^1(S)\text{-4,6-Me}_2\text{DBT})]^+$, rotation around the Ru−S bond is prevented by the close approach (3.076, 3.111 Å) of the 4,6-methyl groups to a

(16) Nakazawa, H.; Kawamura, K.; Kubo, K.; Miyoshi, K. *Organometallics* **1999**, *18*, 2961.

(17) Bruce, M. I.; Zaitseva, N. N.; Skelton, B. W.; White, A. H. *Aust. J. Chem*. **1998**, *51*, 433. The ^{1}H NMR spectrum for the ruthenium product observed was similar to that reported for the cation in $[Cp^*Ru(CO)_2(PPh_3)][Fe_3(\mu_3\text{-}C_2Bu^t)(CO)_9]$.

(18) (a) Benson, J. W.; Angelici, R. J. *Organometallics* **1992**, *11*, 922. (b) Goodrich, J. D.; Nickias, P. N.; Selegue, J. P. *Inorg. Chem.* **1987**, *26*, 3424..

(19) (a) Harman, W. D.; Schaefer, W. P.; Taube, H. *J. Am. Chem. Soc.* **1990**, *112*, 2682. (b) Burns, C. J.; Andersen, R. A. *J. Am. Chem. Soc.* **1987**, *109*, 915.

(20) (a) Fagan, P. J.; Ward, M. D.; Calabrese, J. C. *J. Am. Chem. Soc*. **1989**, *111*, 1698. (b) Polam, J. R.; Porter, L. C. *Inorg. Chim. Acta* **1993**, *205*, 119. (c) Wang, C.-M. J.; Angelici, R. J. *Organometallics* **1990**, *9*, 1770. (d) Xia, A.; Selegue, J. P.; Carillo, A.; Brock, C. P. *J. Am. Chem. Soc*. **2000**, *122*, 3973. (e) Chaudret, B.; Jalon, F. A. *J. Chem. Soc., Chem. Commun.* **1988**, *11*, 711.

(21) The X-ray data showed two structurally independent molecules in the asymmetric unit cell of $[Cp^*Ru(CO)_2(\eta^1(S)\text{-4-MeDBT})]BF_4$. See ref 11.

Table 4. Relative Equilibrium Constants, *K′*, for Reactions of [Cp′Ru(CO)$_2$(η^1(*S*)-4,6-Me$_2$DBT)]$^+$ with DBTh in CD_3NO_2 or CD_2Cl_2 at 25.0 °C

DBTh	[CpRu(CO)$_2$(η^1(*S*)-DBTh)]$^+$ [a]	[Cp*Ru(CO)$_2$(η^1(*S*)-DBTh)]$^+$ [b]
4,6-Me$_2$DBT	1.00	1.00
4-MeDBT	2.79(7)	20.2(1)
DBT	9.71(9)	62.7(6)
2,8-Me$_2$DBT	36.5(3)	223(3)

[a] This study. CD_3NO_2 solvent. [b] Reference 11. CD_2Cl_2 solvent.

plane defined by the Cp* methyl carbon atoms, which restricts the twist angle to only 0.4°. In [Cp*Ru(CO)$_2$-(η^1(*S*)-4-MeDBT)]$^+$, the twist angle is larger (11.3°, 12.3°) and the 4-MeDBT ligand is oriented along the Ru−S bond such that the 4-methyl group is twisted away from the Cp* ligand, reducing the steric interaction between the 4-methyl group and the Cp* methyl groups; distances between the 4-methyl carbon atoms and the Cp* planes are 3.417 and 3.508 Å. An even larger twist angle (22.3°) was observed in [Cp*Ru(CO)$_2$-(η^1(*S*)-DBT)]$^+$, where the distance of closest approach was 3.463 Å; the large twist angle in this complex is presumably controlled by crystal packing forces. The similar values for the distances of closest approach of DBTh carbon atoms in [Cp*Ru(CO)$_2$(η^1(*S*)-4-MeDBT)]$^+$ and [Cp*Ru(CO)$_2$(η^1(*S*)-DBT)]$^+$ to the Cp* planes (3.42−3.51 Å) suggest that those distances are sterically noncrowding. The significantly shorter values in [Cp*Ru-(CO)$_2$(η^1(*S*)-4,6-Me$_2$DBT)]$^+$ (3.076 and 3.111 Å) indicate crowding of the 4,6-Me$_2$DBT methyl groups and the Cp* ligand. Thus, these structural studies show that [Cp*Ru-(CO)$_2$(η^1(*S*)-4,6-Me$_2$DBT)]$^+$ (**7**) is the only complex in the series of either Cp or Cp* [Cp′Ru(CO)$_2$(η^1(*S*)-DBTh)]$^+$ complexes for which there is clear evidence of steric crowding between the 4- or 6-methyl groups on the DBTh and the Cp′ ligands.

Equilibrium Studies. Equilibrium constants (*K*) for the exchange of one dibenzothiophene by another in [CpRu(CO)$_2$(η^1(*S*)-DBTh)]$^+$ were calculated using eq 2, and the values obtained are listed in Table 3. Relative equilibrium constants, *K′* (given in parentheses), for the displacement of 4,6-Me$_2$DBT from [CpRu(CO)$_2$(η^1(*S*)-4,6-Me$_2$DBT)]$^+$ by 4-MeDBT, DBT, and 2,8-Me$_2$DBT are calculated from the experimental *K* values and are listed in Table 4. The *K′* values increase in the order 4,6-Me$_2$-DBT (1.00) < 4-MeDBT (2.79 (7)) < DBT (9.71(9)) < 2,8-Me$_2$DBT (36.5(3)). The larger *K′* value for 2,8-Me$_2$DBT (36.5), as compared to DBT, demonstrates that electron-donating methyl groups in the nonhindering 2,8-positions increase the binding ability of DBT by a factor of 3.8, presumably by making the sulfur atom on DBT a better donor to ruthenium. On the other hand, the 4-MeDBT and 4,6-Me$_2$DBT ligands are only 0.29 and 0.10 times as strongly binding, respectively, as DBT. The first methyl group in the 4-position decreases binding by a factor of 0.29, while a second methyl group in the 6-position reduces the binding even further by a factor of 0.36. Although there is no direct evidence for steric crowding by the 4,6-methyl groups in structural studies of the [CpRu(CO)$_2$(η^1(*S*)-DBTh)]$^+$ complexes, there is clearly an effect on the equilibrium constants. These constants show that the steric effect of the 4,6-methyl groups overrides their increased electron-donating ability.

The relative trend in *K′* values for the DBTh ligands in the [CpRu(CO)$_2$(η^1(*S*)-DBTh)]$^+$ complexes is the same as that reported previously for the [Cp*Ru(CO)$_2$(η^1(*S*)-DBTh)]$^+$ complexes[11] that contain the bulkier η^5-C_5Me_5 ligand (Table 4). As mentioned above, *K′* values for the 2,8-Me$_2$DBT and 4-MeDBT ligands are factors of 3.8 times and 0.29 times, respectively, of that for DBT in the [CpRu(CO)$_2$(η^1(*S*)-DBTh)]$^+$ complexes. These values are very similar to factors of 3.6 times and 0.32 times for 2,8-Me$_2$DBT and 4-MeDBT, respectively, as compared with DBT in the [Cp*Ru(CO)$_2$(η^1(*S*)-DBTh)]$^+$ complexes. The major difference between *K′* values for the Cp and Cp* series of complexes is that between 4,6-Me$_2$DBT and 4-MeDBT. For the Cp complexes (**2** and **3**), 4-MeDBT is 2.8 times more strongly binding than 4,6-Me$_2$DBT. On the other hand, for the Cp* complexes (**6** and **7**), 4-Me$_2$DBT binds *20 times* more strongly than 4,6-Me$_2$DBT. This much larger decrease in the binding ability of 4,6-Me$_2$DBT as compared with 4-MeDBT in the Cp* complexes undoubtedly reflects the substantial steric crowding between the 4,6-Me$_2$DBT methyl groups and the Cp* ligand that was evident in the structural studies.

Table 5. Relative Equilibrium Constants (*K′*) for the Reactions of [CpRu(CO)$_2$(η^1(*S*)-T)]$^+$ with Th at 25.0 °C

Th	*K′*
T[a]	1.00
2-MeT[a]	3.30
3-MeT[a]	4.76
2,5-Me$_2$T[a]	20.7
BT[a,b]	47.6
4,6-Me$_2$DBT[b]	80.9
4-MeDBT[b]	233
DBT[b]	800
Me$_4$T[a]	887
2,8-Me$_2$DBT[b]	3016
THT[a]	>10^5

[a] Reference 14. CD_2Cl_2 solvent. [b] This study. CD_3NO_2 solvent.

Previous work showed that in the series of [CpRu-(CO)(PPh$_3$)(η^1(*S*)-Th)]$^+$ complexes, where Th denotes the thiophene (T), benzothiophene (BT), or dibenzothiophene ligands, relative equilibrium constants (*K′*) follow the order T (1.00) < BT (29.9) < DBT (74.1) < 2,8-Me$_2$DBT (358).[22] A similar study for the [CpRu(CO)$_2$(η^1-(*S*)-Th)]$^+$ complexes revealed the same relative trend for T (1.00) and BT (47.6), but DBT was not examined due to its poor solubility in the chosen CH_2Cl_2 solvent system.[14] To directly compare our results to the previous study undertaken in methylene chloride, three independent reactions of [CpRu(CO)$_2$(η^1(*S*)-BT)]$^+$ and DBT were performed in CD_3NO_2; the *K* was determined to be 0.0597(9). This *K* value allows for the calculation of the relative equilibrium constants listed in Table 5. The weakest ligand in this series is thiophene and the strongest is tetrahydrothiophene (THT). It is clear that

(22) White, C. J.; Wang, T.; Jacobson, R. A.; Angelici, R. J. *Organometallics* **1994**, *13*, 4474.

although methyl groups in the 4- and 6-positions reduce binding of DBT to $\{CpRu(CO)_2\}^+$, 4,6-Me_2DBT is still a better ligand than benzothiophene in this series. This suggests that it should be possible to use metal complexes to remove hindered dibenzothiophenes from diesel fuels by solution phase or solid extraction.

The DBTh binding studies discussed above were the basis for the use of $\{CpRu(CO)_2BF_4\}$ adsorbed on silica-based supports for the removal of dibenzothiophenes from a simulated gasoline/diesel fuel.[8] The adsorbent was created by reacting $CpRu(CO)_2Cl$ with $AgBF_4$ in CH_2Cl_2, filtering the solution onto a solid silica-based support, and evaporating the solution to dryness. Simulated petroleum solutions of DBT and of 4,6-Me_2DBT were then stirred with the solid phase adsorbent. Within 30 min, the sulfur levels were reduced from 400 to 4 ppm for a DBT solution and from 400 to 113 ppm for a 4,6-Me_2DBT solution, corresponding to decreases in the sulfur levels of 96% and 72%, respectively. The less efficient removal of 4,6-Me_2DBT is a direct consequence of methyl groups in the 4,6-positions sterically hindering sulfur coordination to the adsorbent. These results indicate that solution binding studies can be useful in developing new strategies for sulfur removal.

Kinetic Studies of Substitution Reactions of $[Cp'Ru(CO)_2(\eta^1(S)\text{-DBTh})]^+$. Kinetic studies of the reactions of $[Cp'Ru(CO)_2(\eta^1(S)\text{-DBTh})]^+$ with either $P(OPh)_3$, PPh_3, or PPh_2Me according to eq 4 were performed under pseudo-first-order conditions with a minimum of 10-fold excess of PR_3. The pseudo-first-order rate constants, k_{obs}, are listed in Table 6. Plots of k_{obs} versus $[PR_3]$ for the reactions of $[CpRu(CO)_2(\eta^1(S)\text{-DBTh})]^+$ are independent of the PR_3 concentration so that $k_{obs} = k_1$. However, for the $[Cp^*Ru(CO)_2(\eta^1(S)\text{-DBTh})]^+$ complexes, k_{obs} depends partially on the concentration of the phosphine such that $k_{obs} = k_1 + k_2[PR_3]$. The k_1 values for both series of complexes are given in Table 7.

The first-order rate law indicates that the reaction of $[CpRu(CO)_2(\eta^1(S)\text{-DBTh})]^+$ with $P(OPh)_3$ proceeds by a mechanism involving slow dissociation of the DBTh ligand followed by rapid reaction of the unsaturated intermediate with $P(OPh)_3$ to give the final product. The k_1 values for these reactions, listed in Table 7, decrease with the DBTh ligand in the following order: 4,6-Me_2DBT ($5.18(5) \times 10^{-6}$ s^{-1}) > 4-MeDBT ($4.50(3) \times 10^{-6}$ s^{-1}) > DBT ($4.01(3) \times 10^{-6}$ s^{-1}) > 2,8-Me_2DBT ($1.33(5) \times 10^{-6}$ s^{-1}). This trend parallels the trend observed in the equilibrium studies (Table 4), which shows that the more strongly binding the DBT ligand thermodynamically, the slower its rate of dissociation from $[CpRu(CO)_2(\eta^1(S)\text{-DBTh})]^+$. The rate of dissociation of the 2,8-Me_2DBT ligand is a factor of 0.33 as fast as that of DBT. Thus, electron-donating methyl groups located away from the sulfur atom in 2,8-Me_2DBT not only increase the thermodynamic stability of the Ru−S bond, as the equilibrium studies indicate, but also decrease the kinetic lability of the Ru−S bond. On the other hand, the rates of dissociation of the 4-MeDBT and 4,6-Me_2DBT ligands are 1.13 and 1.30 times faster, respectively, than that of DBT. The steric effects of methyl groups in the 4,6-positions of DBT outweigh their electron-donating effects, which results in lower thermodynamic stabilities and greater kinetic labilities of the Ru−S bond in the 4-MeDBT and 4,6-Me_2DBT complexes.

Table 6. Rate Constants, k_{obs} (s^{-1}), for Reactions (eq 4) of 0.020 M $[Cp'Ru(CO)_2(\eta^1(S)\text{-DBTh})]^+$ with PR_3 at 25.0 °C

DBTh	PR_3	$[PR_3]$, M	$10^6 k_{obs}$, s^{-1}
	$[CpRu(CO)_2(\eta^1(S)\text{-DBTh})]^+$ [a]		
4,6-Me_2DBT	PPh_3	0.10	5.21
		0.20	5.30
		0.30	5.28
		0.40	5.25
	$P(OPh)_3$	0.20	5.21
		0.60	5.07
		1.00	5.25
4-MeDBT	$P(OPh)_3$	0.20	4.47
		0.60	4.54
DBT	$P(OPh)_3$	0.20	3.97
		0.20	4.03
		0.60	4.02
2,8-Me_2DBT	$P(OPh)_3$	0.20	1.32
		0.20	1.28
		1.00	1.38
	$[Cp^*Ru(CO)_2(\eta^1(S)\text{-DBTh})]^+$ [b]		
4,6-Me_2DBT	PPh_3	0.20	475
		0.40	517
		0.60	548
		1.00	600
DBT	PPh_3	0.20	131
		0.40	150
		0.60	169
		0.80	183
		1.00	201
	PPh_2Me	0.20	139
		0.60	175
		0.80	194
		1.00	214
4-MeDBT	PPh_3	0.20	71.0(5)
		0.40	77.4
		0.60	84.1
		0.80	91.4
		1.00	98.2
	PPh_2Me	0.20	71.1
		0.40	78.0
		0.60	85.9
		0.80	97.8
		1.00	101
2,8-Me_2DBT	PPh_3	0.20	29.2
		0.40	35.1
		0.60	38.9
		0.80	42.5
		1.00	44.0

[a] CD_3NO_2 solvent. [b] CD_2Cl_2 solvent.

When PPh_3 was used as the incoming ligand (eq 4), $[CpRu(CO)_2(\eta^1(S)\text{-4,6-}Me_2DBT)]^+$ reacted cleanly to give $[CpRu(CO)_2(PPh_3)]^+$, whose ^1H NMR spectrum was nearly identical to that reported previously for this compound.[23] Due to the relative insolubility of PPh_3 in CD_3NO_2, reaction solutions containing only 10-, 15-, and 20-fold excess of PPh_3 were possible. The rates of these reactions were independent of the PPh_3 concentration (Table 6), and the k_1 rate constant was the same within experimental error as that with $P(OPh)_3$ (Table 7). However, reactions of the DBT (**1**) and 4-MeDBT (**2**) complexes with PPh_3 resulted in the formation of two phosphine products within 12 h: $[CpRu(CO)_2(PPh_3)]^+$ and a product whose ^1H NMR spectrum was similar to that reported for $[CpRu(CO)(PPh_3)_2]^+$.[24] Qualitatively,

(23) (a) Davies, S. G.; Simpson, S. J. *Dalton Trans.* **1984**, 993. (b) Humphries, A. P.; Knox, S. A. R. *Dalton Trans.* **1975**, 1710.

(24) Stone, F. G. A.; Blackmore, T.; Bruce, M. I. *J. Chem. Soc., A* **1971**, 2376.

Table 7. First- and Second-Order Rate Constants, k_1 and k_2, for the Substitution of DBTh in $[Cp'Ru(CO)_2(\eta^1(S)\text{-DBTh})]^+$ by PR_3 (eq 4) at 25.0 °C

	$[CpRu(CO)_2(\eta^1(S)\text{-DBTh})]^{+,a}$	$[Cp^*Ru(CO)_2(\eta^1(S)\text{-DBTh})]^{+,b}$	
DBTh	$10^6\,k_1$, s^{-1}	$10^6 k_1$, s^{-1}	$10^6 k_2$, $M^{-1}\,s^{-1}$
4,6-Me_2DBT	5.18(10),[c] 5.26(4)[d]	451(±8)[d]	152(±13)[d]
4-MeDBT	4.50(3)[c]	63.9(±0.3),[d] 62.7(±2.1)[e]	34.2(±0.4),[d] 40.2(±3.2)[e]
DBT	4.01(3)[c]	115(±2),[d] 120(±2)[e]	86.5(±2.8),[d] 93.0(±1.6)[e]
2,8-Me_2DBT	1.33(5)[c]	26.8(±1.5)[d]	18.5(±2.2)[d]

[a] In CD_3NO_2. [b] In CD_2Cl_2. [c] For $PR_3 = P(OPh)_3$. [d] For $PR_3 = PPh_3$. [e] For $PR_3 = PPh_2Me$.

this reaction occurred more rapidly and more of the second phosphine product was formed in the reactions of the DBT complex (**1**) than the 4-MeDBT complex (**2**). Because these reactions yielded two products, their kinetics were not investigated further.

The k_{obs} rate constants for reactions of the $[Cp^*Ru(CO)_2(\eta^1(S)\text{-DBTh})]^+$ complexes with PPh_3 and PPh_2Me show (Table 6) a small but discernible contribution from a second-order (k_2) pathway in addition to the k_1 pathway. The k_1 values for the reactions of $[Cp^*Ru(CO)_2(\eta^1(S)\text{-DBTh})]^+$ with PPh_3 decrease in the following order: 4,6-Me_2DBT ($(451 \pm 8) \times 10^{-6}$ s^{-1}) > DBT ($(115 \pm 2) \times 10^{-6}$ s^{-1}) > 4-MeDBT ($(63.9 \pm 0.3) \times 10^{-6}$ s^{-1}) > 2,8-Me_2DBT ($(26.8 \pm 1.5) \times 10^{-6}$ s^{-1}). The reactions of $[Cp^*Ru(CO)_2(\eta^1(S)\text{-DBT})]^+$ and $[Cp^*Ru(CO)_2(\eta^1(S)\text{-MeDBT})]^+$ with PPh_2Me yielded k_1 values ($(120 \pm 2) \times 10^{-6}$ s^{-1} for DBT and $(62.7 \pm 2.1) \times 10^{-6}$ s^{-1} for 4-MeDBT) that were the same within experimental error as those determined using PPh_3. The rate-determining step for the k_1 pathway in the reactions of the $[Cp^*Ru(CO)_2(\eta^1(S)\text{-DBTh})]^+$ complexes with both PPh_3 and PPh_2Me is likely dissociation of the DBTh ligand. As for the $[CpRu(CO)_2(\eta^1(S)\text{-DBTh})]^+$ complexes, the rates for three of the four $[Cp^*Ru(CO)_2(\eta^1(S)\text{-DBTh})]^+$ complexes decrease as follows: 4,6-Me_2DBT > DBT > 2,8-Me_2DBT. Steric and electronic factors account for this trend, as discussed above. On the other hand, the 4-MeDBT ligand in $[Cp^*Ru(CO)_2(\eta^1(S)\text{-MeDBT})]^+$ (**6**) dissociates *more slowly* than DBT from $[Cp^*Ru(CO)_2(\eta^1(S)\text{-DBT})]^+$, which is different than the trend in rates for the $[CpRu(CO)_2(\eta^1(S)\text{-DBTh})]^+$ complexes and different than the trend in equilibrium binding constants (Table 4) for both series of $[Cp'Ru(CO)_2(\eta^1(S)\text{-DBTh})]^+$ complexes. To explain the anomalously slow rate of 4-MeDBT dissociation from **6**, one can propose that the low-energy pathway for 4-MeDBT dissociation is one in which the DBTh ligand is oriented so that the complex has a plane of symmetry; that is, the complex has a 0° twist angle. The 4,6-Me_2DBT complex is forced by steric factors to have this orientation, and the DBT and 2,8-Me_2DBT ligands can easily achieve this orientation by rotation around the Ru−S bond. However, there will be a barrier to achieving this orientation with the 4-MeDBT ligand because of steric repulsion between the 4-methyl group and the Cp* methyl groups, which may account for the unexpectedly slow rate of 4-MeDBT dissociation from complex **6**.

The k_1 values for the $[Cp^*Ru(CO)_2(\eta^1(S)\text{-DBTh})]^+$ complexes are all significantly greater than those determined for the $[CpRu(CO)_2(\eta^1(S)\text{-DBTh})]^+$ complexes. For example, the rate of dissociation of DBT is 29 times faster in the Cp* complex (115×10^{-6} s^{-1}) as compared with that in the Cp complex (4.01×10^{-6} s^{-1}). Since there is little steric influence in both the Cp and Cp* complexes of DBT, the faster rate for the Cp* complex presumably is a result of the greater electron-donating ability of the Cp* ligand. The added electron density reduces the Lewis acidity of the Ru atom, which weakens the Ru−S bond and makes the DBT ligand more labile in $[Cp^*Ru(CO)_2(\eta^1(S)\text{-DBT})]^+$ (**5**) as compared to the Cp complex **1**. The dissociation rate of 4-MeDBT from $[Cp^*Ru(CO)_2(\eta^1(S)\text{-4-MeDBT})]^+$ is 14 times faster than that from its Cp analogue, and the rate for 2,8-Me_2DBT dissociation from $[Cp^*Ru(CO)_2(\eta^1(S)\text{-2,8-}Me_2\text{DBT})]^+$ is 20 times faster than that from its Cp analogue. The increases in the kinetic labilities of the 4-MeDBT and 2,8-Me_2DBT ligands in the Cp* complexes as compared with the Cp complexes are also likely a result of the greater electron-donating ability of the Cp* ligand as described for DBT above. On the other hand, the dissociation rate of 4,6-Me_2DBT from $[Cp^*Ru(CO)_2(\eta^1(S)\text{-4,6-}Me_2\text{DBT})]^+$ (**7**) is *86 times* its rate of dissociation from $[CpRu(CO)_2(\eta^1(S)\text{-4,6-}Me_2\text{DBT})]^+$. This much larger rate of dissociation of 4,6-Me_2DBT in the Cp* complex (**7**) than in its Cp analogue (**3**) is due not only to the higher electron-donating ability of Cp* but also to the steric effect of the more bulky Cp* ligand. On the basis of the above comparisons, the electronic effect of the Cp* ligand increases the rate of 4,6-Me_2DBT dissociation from **7** by a factor of approximately 20, which means that the rate enhancement caused by steric erepulsion is a factor of approximately 4.

The k_2 values obtained from the plots of k_{obs} versus phosphine concentration for the reactions of the $[Cp^*Ru(CO)_2(\eta^1(S)\text{-DBTh})]^+$ complexes with PPh_3 and PPh_2Me are listed in Table 7. The k_2 values for the reaction with PPh_3 decrease in the same order as the k_1 values: 4,6-Me_2DBT ($(152 \pm 13) \times 10^{-6}$ s^{-1}) > DBT ($(86.5 \pm 2.8) \times 10^{-6}$ s^{-1}) > 4-MeDBT ($(34.2 \pm 0.4) \times 10^{-6}$ s^{-1}) > 2,8-Me_2DBT ($(18.6 \pm 2.2) \times 10^{-6}$ s^{-1}). The similarity of the trends in k_1 and k_2 values suggests that Ru−S bond-breaking primarily determines the overall rate of the second-order reaction. That bond-making with the incoming PR_3 ligand is less important is indicated by the fact that the k_2 values for PPh_3 and PPh_2Me in their reactions with **5** and **6** are nearly the same (Table 7). If the mechanism were to involve nucleophilic attack of the phosphine on the Ru, one would expect a much larger difference in their rates.[25] Thus, the mechanism for the k_2 pathway is best described as a dissociative interchange (I_d) where the nature of the $[Cp^*Ru(CO)_2(\eta^1(S)\text{-DBTh})][BF_4]\cdot PR_3$ intermediate is not clear. It should be noted that this I_d pathway contributes to the total rate only at relatively high concentrations of the phosphine.

Conclusions

Investigations of the two series of dibenzothiophene complexes $[Cp'Ru(CO)_2(\eta^1(S)\text{-DBTh})]^+$, where Cp′ = Cp

(25) Poe, A. J. *Pure Appl. Chem.* **1988**, *60*, 1209.

or Cp*, show that only in the structure of $[Cp^*Ru(CO)_2(\eta^1(S)\text{-}4,6\text{-}Me_2DBT)]^+$ is there evidence for steric crowding between methyl groups in the 4,6-Me_2DBT and Cp* ligands. This effect is also evident in the equilibrium binding constants (K') for the coordination of 4,6-Me_2DBT to $\{Cp^*Ru(CO)_2\}^+$, which are much smaller than those for 4-MeDBT. In both series of complexes, both steric and electronic factors affect the K' values, which increase in the order 4,6-Me_2DBT < 4-MeDBT < DBT < 2,8-Me_2DBT. The rates of DBTh substitution by PR_3, following a dissociative mechanism, are especially fast for the sterically crowded $[Cp^*Ru(CO)_2(\eta^1(S)\text{-}4,6\text{-}Me_2DBT)]^+$, but steric and electronic effects also contribute to the rates of substitution of the other DBTh ligands.

Acknowledgment. This work was supported by the U.S. Department of Energy, Office of Science, Office of Basic Energy Sciences, Chemical Sciences Division, under contract W-7405-Eng-82 with Iowa State University.

Supporting Information Available: Crystallographic files (CIF) and tables giving crystallographic data for complexes **2**, **3**, and **4**, including atomic coordinates, bond lengths and angles, and anisotropic displacement parameters. This material is available free of charge via the Internet at http://pubs.acs.org.

OM048973L